

SPONTANEOUS CO₂ EMULSION GENERATION; A NEW APPROACH FOR MOBILITY CONTROL

Alireza Emadi¹ and Mehran Sohrabi

Centre for Enhanced Oil Recovery and CO₂ Solutions,
Institute of Petroleum Engineering, Heriot-Watt University, Edinburgh, UK

*This paper was prepared for presentation at the International Symposium of the Society of
Core Analysts held in Napa Valley, California, USA, 16-19 September, 2013*

ABSTRACT

Formation of stable dispersions of CO₂ in aqueous phase (e.g. CO₂-foam or emulsion), improves the performance of CO₂ injection by reducing its mobility. The effectiveness of this process to a large extent depends on sufficient formation of dispersion bubbles and their stability in the reservoir. This paper presents the results of an integrated direct flow visualisation (micromodel) and coreflood study, in which spontaneous in-situ formation of liquid CO₂ dispersions as a new and effective technique for mobility control in oil reservoir is investigated.

The first set of experiments was performed using clean (oil-free) porous media. The results of coreflood tests showed a substantial drop in CO₂ mobility due to simultaneous injection of liquid CO₂ and a surfactant solution. The apparent viscosity achieved from simultaneous injection of liquid CO₂ and the surfactant solution was dramatically higher than similar tests in which vapour and super-critical (SC) CO₂ were used with the same surfactant solution. The observations from micromodel tests showed that the observed exceptional performance of liquid CO₂ is due to spontaneous nucleation and formation of a large number of liquid CO₂ droplets (emulsions) in the porous media which was not the case during vapour and SC CO₂ injection.

The second set of experiments was performed to investigate the impact of crude oil on spontaneous formation and stability of CO₂-emulsion. The results of the coreflood tests showed formation of a stable CO₂-emulsion that efficiently reduced CO₂ mobility even at high oil saturations of near 50%. The micromodel experiments showed that while presence of oil reduces the stability of CO₂ emulsions, at the same time, it accelerates their spontaneous nucleation and formation which provides a state of semi-equilibrium between the rate of generation and the rate of termination of CO₂ bubbles. This can potentially eliminate one of the main restrictions of field application of CO₂-foam (emulsion) injection.

¹ Now in Corex UK Ltd.

INTRODUCTION

CO₂ injection is a well-researched and established oil recovery technique that has been utilized in different types of reservoirs to enhance oil recovery. The main benefits of CO₂ come from mass exchange between CO₂ and oil which may result in miscible or immiscible displacement processes. In a miscible displacement process, the elimination of capillary forces at the CO₂ front makes the pore-scale displacement very efficient. As injection of CO₂ continues, the remaining oil behind the main CO₂ front continues producing by diffusive mechanisms. However, even if miscibility is not attained, other mechanisms driven by the dissolution of CO₂ into the oil phase, including oil swelling and viscosity reduction and/or vaporization of hydrocarbon components into the CO₂ phase, can significantly improve oil recovery (Klins and Bardon 1991). Nevertheless, the adverse viscosity ratio between CO₂ and oil remains a serious drawback for CO₂ flood process. This causes viscous fingering and early breakthrough of CO₂ in both miscible and immiscible displacement scenarios. Formation of stable dispersions of CO₂ in aqueous phase (e.g. CO₂ foam) is one of the most effective techniques that have been applied in order to improve sweep efficiency of CO₂.

Mobility of foam in porous media is many orders of magnitude smaller than that of the constituent gas and liquid. The mobility reduction is achieved primarily because the gas phase is dispersed into small bubbles (foam), which are generally about the size of the pore channels. Consequently, bubble interactions with pore walls dominate foam flow behaviour in porous media. For this reason, the pressure drop/flow rate relationship of foam in porous media depends strongly on the texture of the foam (Chambers and Radke 1990).

Technically, there are two approaches to the application of foam for improved oil recovery (IOR). The simplest is to plug unwanted reservoir layers and regions near an injection or production well with relatively small volumes of foam. Oil saturation in near-wellbore regions of injection wells is generally low (as a result of higher velocities of fluids); therefore, most of the laboratory experiments are performed without (or at low) oil saturation if the near-wellbore application of foam is desired. However, diverting flow in the near-well region may not affect flow patterns in the bulk of the reservoir. The more ambitious goal is “mobility control” throughout the entire formation. This latter approach (that is the subject of this study) requires formation of a foam-filled region spanning large distances over periods of months or years. It has a potential to redirect flow patterns throughout the reservoir and greatly increase oil recovery (Rossen 1995). The critical aspect of such processes is the propagation of foam in oil filled porous media. This requires the rate of foam generation to be equal or higher than the rate of foam decay. Therefore, detailed studies of generation and termination mechanisms at pore scale and the effect of oil on bubble stability are essential to evaluate propagation of foam/emulsion throughout the reservoir.

It is commonly accepted that lamellae (or foam bubbles) are created by the following three mechanisms inside a realistic porous media:

- 1) “Leave behind” is creation of stabilized liquid films lenses in pore throats as gas invades adjacent pore bodies through other throats. Although sometimes cited as a source of “weak” foam, the leave behind mechanism can create a large number of lamellae. However, if it is the only lamella creation mechanism, the gas will always have at least one continuous pathway for flow (Chen et al. 2006).
- 2) “Lamella division” denotes the event when two or more lamellae are created from a single one. Each time a mobilized lamella passes a pore body, with more than one pore throat unoccupied with liquid or another lamellae, this must either break or span both open throats (Rossen 1995).
- 3) “Snap-off” is a third mechanism for lamella generation: lamellae are created in gas-filled pore throats, if the local capillary pressure falls to about half the capillary entry pressure of the throat. While it depends on the geometry of the throat and the wettability of the medium, the value of one-half is a reasonable representative value for three dimensional (3D) pore geometries (Chen et al. 2006).

There are a number of mechanisms that can result in destabilization of foam in porous media through physical and chemical interactions.

- 1) Capillary Suction Coalescence: Moving lamellae coalesce when they are rapidly stretched across large pore bodies. For a given gas flow rate and capillary pressure, pore-throat/pore body combinations with large aspect ratios, serve as termination sites. As the gas velocity and /or porous medium capillary pressure increases, more and more throat/body configurations become termination sites (Chambers and Radke 1990).
- 2) Gas diffusion Coalescence: Trapped or static bubbles break by a second mechanism. Whenever two bubbles with different curvatures are in contact, gas diffuses from the more highly curved bubbles (smaller bubbles) to the less curved bubbles (bigger bubbles) through the intervening lamellae. Eventually, the smaller bubbles disappear along with the common lamellae (Chambers and Radke 1990).
- 3) Destabilisation by oil: The oil may spontaneously spread on foam lamellae, displacing the elastic stabilizing interface; or the oil may spontaneously emulsify, allowing drops to breach (enter) and rupture the stabilizing interface. (Schramm and Novosad 1990). It should be noted that the presence of oil not only causes destabilization of foam but also reduces the rate of foam generation as it is decreasing the interfaces between gas and surfactant solution.
- 4) Chemical destabilization: Surfactants may be absorbed to rock and oil, causing depletion of the surfactant from the aqueous phase and gas/liquid interface; or surfactants from the oil may be absorbed by the lamellae, producing a less favourable state for foaming. These phase-behaviour changes are usually negligible for the commercial foam forming surfactant (Schramm and Novosad 1990).

Various parameters have been identified in the literature which can influence formation of strong foam in porous media. Flow rate and oil saturation are two of the most important parameters which partially control generation and destabilization of foam bubbles. Various researchers have reported a critical oil saturation (around 15%) above which it is very difficult to produce strong foam in porous media (Svorstol et al. 1996). This is because oil destabilizes foam bubbles and at the same time slows down formation of new bubbles as was explained earlier. Reported laboratory results also show that strong foam, which can effectively reduce mobility of gas, is formed only above a critical injection velocity (or pressure gradient). Rossen and Gauglitz (1990) argue that a minimum injection velocity is required to displace lamellae out of pore throats and produce flowing foam. Only flowing foam can effectively reduce mobility of gas in porous media.

In real reservoir conditions, when injected fluids pass the near wellbore region to enter reservoir region, there is a transition zone in which the velocity of fluid flow dramatically drops and oil saturation increases (to around 40% in swept regions and higher oil saturations in unswept regions of the reservoir). This means, while strong foam can be generated in the near wellbore region due to high flow rates and low oil saturation, it will be easily destabilized when it enters the reservoir region. This may result in complete decay of foam only hundreds of feet away from the injection well. This study identifies and introduces a new type of CO₂ droplet/bubble generation mechanism that is not rate dependent and can produce stable foam/emulsion deep in the reservoir region.

It should be noted that similar concepts and definitions to that of CO₂-foam has been utilized for CO₂-emulsion (using liquid CO₂) in this study with the exception that the terminology of 'foam bubbles' is replaced by 'emulsion droplets'.

EXPERIMENTAL FACILITIES

Micromodel Tests

A high-pressure micromodel rig was used to perform the direct observation experiments. Details of the rig can be found in one of our previous publications (Sohrabi et al. 2000). In this study, a homogenous rock-look-like pattern micromodel was used. The micromodel orientation was vertical with the inlet port at the top and the outlet at the bottom end of the model. Table 1 shows the dimensions of the micromodel and their pores.

Coreflood Tests

A high pressure coreflood facility was used to perform the displacement and mobility control tests. Details of this coreflood rig can be found elsewhere (Emadi et al. 2013). The coreflood experiments were all conducted using a highly permeable core sample of Fife silica-sand, taken from central Scotland. This high purity sandstone typically contains less than 2% feldspar and clay content. A summary of the core properties is

given in Table 2. The coreholder was mounted vertically and injection of fluids commenced from top end of the core.

Fluids

Table 3 presents the basic properties of the viscous crude oil used in the micromodel and coreflood experiments. A synthetic brine containing both NaCl and CaCl₂ salts was prepared and used in the coreflood tests as connate water. This brine was also used to produce the surfactant solution. The brine had a total dissolved salt concentration of 10000 ppm consisting of 8000 ppm NaCl and 2000 ppm CaCl₂. In the micromodel tests, the brine was replaced with distilled water. The brine and distilled water were de-aired before injection into the storage cell. The CO₂ used in the tests was provided in a highly purified form of 99.8%. CO₂ is present in liquid state at the conditions of the reservoir from which the heavy crude oil was taken. The properties of the liquid CO₂ used in this study are listed in Table 4 and are compared to that of gaseous CO₂ and distilled water. As can be seen, the density of liquid CO₂ is similar to density of water however its viscosity is still significantly lower than that of water. The surfactant used in this study was an anionic surfactant which is referred to as “HW-A”.

EXPERIMENTAL PROCEDURE

Lists of the coreflood and micromodel tests and their descriptions are provided in Tables 5 and 6, respectively. To prepare the core and micromodel for testing, the system was cleaned with copious amounts of toluene and methanol injected in succession. Both core and micromodel were housed vertically and all fluids were injected from the top end of the system. To simulate a displacement process at reservoir conditions, the injection rate was selected such that a frontal velocity similar to that of real field conditions (few feet per day) could be achieved. In the coreflood experiments, the total injection rate was set to 7 cc/hr providing a frontal velocity of 1 ft/hr. The capillary number was calculated to be 1.5E-7 during displacement of oil by water which shows a capillary dominant displacement in the porous media. The capillary number definition used here is similar to that defined by Green and Willhite (1986) without considering the term of wettability ($\cos \theta$), as:

$$N_{ca} = \frac{v\mu_D}{\sigma}$$

Where; “ μ_D ” is the displacing phase viscosity, “ v ” is the pore velocity, and “ σ ” is the surface tension or IFT between the two fluid phases. For micromodel tests the total injection rate was set to 0.01 cc/hr representing a capillary number of around 2.5E-7 for oil/water displacement tests.

RESULTS

CO₂-Emulsion Performance in Absence of Oil

In the first set of experiments, formation of foam/emulsion in clean porous media (in absence of oil) was investigated. Three coreflood experiments were performed using vapour, SC and liquid CO₂ to measure apparent viscosity of the in-situ generated CO₂

foam/emulsion with the selected surfactant. The core was initially saturated with the surfactant solution and then CO₂ and surfactant solution were injected simultaneously through the core with the ratio of 4.5/2.5 for CO₂ and surfactant solution, respectively. Figure 1 presents the apparent viscosity of CO₂ foam/emulsion during this period of CO₂/surfactant injection. In the first test using vapour CO₂ at pressure and temperature of 600 psig and 28 C, the viscosity of in-situ generated foam was around 4 cp which was 4 times higher than that of the aqueous phase. In the second experiment, similar injection procedures were used but at pressure and temperature of 1500 psig and 50 C where CO₂ is in SC form. The results showed an apparent viscosity of around 40 cp which was an order of magnitude higher than that of the foam produced using vapour CO₂ and 50 times higher than that of the aqueous phase. It should be noted that the relatively low apparent viscosity of in-situ generated foam in this test and the previous one is due to maintaining the flow rate at a low level similar to that of the reservoir to achieve a frontal velocity of 1 foot per day. At higher flow rates, both vapour and SC CO₂ produce very stable foam with this foaming agent. In the third coreflood test, liquid CO₂ was used at pressure and temperature of 1500 psig and 28 C. The results of this test showed a dramatic increase in differential pressure across the core corresponding to foam viscosities of close to 3000 cp. This is more than three orders of magnitude higher than that of the aqueous phase and two orders of magnitude more than that of SC CO₂. This means that the foam/emulsion generation mechanisms are significantly faster in Test 3 compared to Test 1 and Test 2 which results in stronger foam/emulsion in porous media and higher viscosity.

To investigate the interactions between CO₂ and surfactant at pore scale, the coreflood experiments were duplicated using micromodel. Initially, the micromodel was fully saturated with surfactant solution and then CO₂ and surfactant were simultaneously injected. When the front of CO₂ reached the middle of the micromodel, injection was stopped in order to further study the size and number of foam/emulsion bubbles in the porous media. The result of the micromodel tests showed that lamellae division was the dominant bubble generation mechanism at the pore scale. The rate of bubble generation by the lamellae division mechanism was higher in liquid CO₂ compared to gaseous (vapour and SC) CO₂ which can be related to the difference in IFT and differences in other physical properties of CO₂. This can partially explain the dramatic increase in apparent viscosity of CO₂ emulsion compared to CO₂ foam. However, an important observation was formation of a large number of small size bubbles around the mainstream of liquid CO₂ when there was no fluid flow in the system. Spontaneous formation of CO₂ emulsions started around bubbles of CO₂ and then extended to other regions of the micromodel. The number of spontaneously generated CO₂ droplets was higher around the CO₂ front compared to other regions of the micromodel that had already been flooded with CO₂. This might be due to a higher rate of mass transfer between CO₂ and aqueous phase at CO₂ front. Formation of a large number of CO₂ micro-emulsions can be clearly seen in Figure 2 where the mixture of liquid CO₂ and surfactant was stationary (static) for a period of two hours.

The process of formation of CO₂ emulsions started by formation of small nucleates which grew larger with time. However, their size did not exceed the size of the pores in which they were located. This means that the droplets that were formed by this mechanism did not spread into more than one pore body. It should be mentioned that spontaneous formation of CO₂ emulsions was also active during the initial CO₂ flow period; however, it was better recognized when fluid flow stopped in the system as other bubble/droplet generation mechanisms were flow dependent and they ceased producing CO₂ droplets when injection stopped.

CO₂-Emulsion Performance in Presence of Oil

The results of previous experiments showed that simultaneous injection of liquid and surfactant solution results in formation of a strong CO₂-emulsion in clean porous media. The high strength of in-situ generated CO₂-emulsion is believed to be at least partially due to spontaneous formation of a large number of CO₂ droplets. However, the question is whether spontaneous formation of CO₂ emulsions takes place in presence of oil. To investigate the interactions of the surfactant and liquid CO₂ in presence of oil, a new micromodel test was conducted in which the process of oil displacement by tertiary CO₂-emulsion flood was physically simulated and visually studied.

In this test, the micromodel was initially saturated with water and then was flooded with oil to establish initial water and oil saturation. To simulate waterflooding of an oil reservoir, the model was then flooded with water for an extended period of time. The test continued with injection of a pre-flush of surfactant and then simultaneous injection of CO₂ and surfactant was started. An important observation was that the presence of oil not only did not adversely affect spontaneous formation of CO₂ droplets but, on the contrary, promoted their generation and their growth rate. The CO₂ droplets were mainly formed at the oil/surfactant solution interface. Figure 3 shows a sequence of highly magnified images of a section of the micromodel when CO₂-emulsion front comes in contact with residual oil. It can be seen that as soon as the CO₂ comes close to the oil blobs, nucleation of CO₂ droplets begin at the oil/surfactant solution interfaces and, in only six seconds, nine new droplets of CO₂-emulsion are spontaneously formed. The observations show that the rate of spontaneous generation and growth of CO₂ droplets in the presence of oil is orders of magnitude higher than in a clean system (Figure 2).

Figure 4 shows a magnified image of a section of the CO₂-emulsion front. As can be seen, there are a large number of small CO₂ droplets which are flowing (not stationary) in the porous media. Formation of small-size emulsions (smaller than size of pore bodies) is only possible through the spontaneous emulsification mechanism as other mechanisms of CO₂ emulsion generation (lamellae division and snap-off) result in formation of bubbles/droplets which are the same size as or larger than pore bodies. It should be noted that while the presence of oil accelerated spontaneous nucleation and formation of CO₂-emulsion, at the same time the other CO₂-emulsion generation

mechanisms (leave behind, lamellae division and snap-off) were slowed down. Additionally, in the areas with high residual oil saturation, oil destabilized the CO₂-emulsion droplets by spreading around CO₂ droplets.

To quantify the observations in the micromodel tests and examine the effect of oil on mobility control by CO₂-emulsion, two new coreflood tests were performed. In the first test, liquid CO₂ and the surfactant solutions were simultaneously injected in the core after an initial period of waterflood. In the second test, very similar procedures were followed; however, this time the period of waterflood was followed by only liquid CO₂ injection. Based on the results of these two experiments, the performance of liquid CO₂ flood and CO₂-emulsion flood processes, in terms of recovery improvement and mobility control, can be compared.

Figure 5 demonstrates the cumulative oil recovery curve during the initial waterflood and the subsequent liquid CO₂/surfactant injection in Test 4. As can be seen, the initial waterflood resulted in an early breakthrough (BT), recovering 16% OOIP. The recovery increased to 28% OOIP after 2 pore volumes (PV) of waterflood. After the initial period of waterflood, the test continued with co-injection of CO₂ and surfactant from the top end of the core. At the early stages of CO₂/surfactant injection, before the CO₂ breakthrough, the core effluent mostly consisted of brine and oil at high water cut (around 0.95). Brine production was followed by production of a small bank of crude oil (3% OOIP) before CO₂ BT which took place after 0.21 PV of CO₂/surfactant co-injection. Oil production after CO₂ BT continued at high rates increasing the oil recovery of 28% OOIP at the end of waterflood to 31%, 46% and 56% OOIP after CO₂ BT, 0.5 and 1 PV of CO₂/surfactant co-injection, respectively. The recovery of 56% OOIP after 1 PV of CO₂/surfactant injection is twice the recovery of the initial waterflood. It should be noted that, in this test, injection of a pre-flush of surfactant solution was not performed in order to provide better comparison between the performance of CO₂ emulsion and that of liquid CO₂ (next test). Injection of pre-flush of CO₂ is expected to significantly improve formation of CO₂ emulsions in-situ and improve recovery and mobility control in the system.

In Test 5, a procedure similar to that of Test 4 was followed; however, this time after the initial period of waterflood, only CO₂ was injected in the system instead of co-injection of CO₂ and surfactant. Comparison of the oil recovery data of this test and previous tests should show if the high oil recovery and good performance of CO₂/surfactant injection was a result of the mechanisms associated with CO₂ injection, e.g. swelling and viscosity reduction, or if formation of stable CO₂-emulsions (due to spontaneous nucleation) is the main mechanism responsible for additional recovery. Figure 6 compares the measured additional oil recovery by CO₂ and CO₂-emulsion (both injected in tertiary mode) which shows much better performance for the CO₂-emulsion process, especially at early injection times. Co-injection of CO₂/surfactant (CO₂-emulsion injection process) produced almost 24% of the Sorw (residual oil in the

core) after 0.4 PV injection. The additional recovery at the same volume of CO₂ injection was around 12% of Sorw.

While the results of Test 4 show that co-injection of CO₂/surfactant has been very successful in terms of promoting oil recovery, formation of a strong CO₂-emulsion needs to be confirmed by comparison of the differential pressure data. Figure 7 compares the differential pressure across the core during the period of tertiary liquid CO₂ injection in Test 5 and CO₂-emulsion injection in Test 4 which indicates excellent mobility control by CO₂-emulsion. As can be seen, the increasing trend in differential pressure during CO₂/surfactant co-injection started at oil saturations around 50%. At oil saturations between 40 to 45%, the differential pressure of the CO₂-emulsion test was one order of magnitude higher than that of CO₂ injection. Also, the difference in differential pressure increased to two orders of magnitude at oil saturations between 30% and 35% indicating formation of strong CO₂-emulsion in the system.

DISCUSSIONS

The micromodel observations in this study show spontaneous formation of droplets of CO₂-emulsion in a specific surfactant solution when the system is in no-flow condition. This is against the theory of foam destabilization by capillary suction mechanisms, as was described in the introduction section of this paper, and is not yet fully understood. While the thermodynamics of this process requires further investigation, the immediate effect of such process would be formation of stronger foam and emulsion in the porous media as was seen during liquid CO₂ and surfactant co-injection in the coreflood test.

Unlike other foam/emulsion generation mechanisms, spontaneous formation of droplets of CO₂-emulsions is not dependent on the pressure gradient or fluid velocity in the system. It means that this process takes place even when CO₂ and surfactant are flowing at very low rates in the reservoir. However, the rate of spontaneous nucleation and growth is higher in the places that rate of mass transfer (by diffusion) is also higher, e.g. interface of CO₂ with unsaturated surfactant solution, as was observed in Test 3. Also, spontaneous formation of droplets of CO₂-emulsion is not sensitive to the presence of oil. On the contrary, the process speeds up when residual oil is present in porous media. These two characteristics (not dependent on fluid velocity and not adversely affected by presence of oil) make it a suitable and efficient technique for formation of emulsions and mobility control in the body of the reservoir where fluid displacement takes place at very slow rates and in the presence of oil.

The most critical aspect of designing a system with spontaneous generation of CO₂ bubbles/droplets is the design of the surfactant solution. Our observations so far show that only specific types of surfactants are able to spontaneously generate CO₂ bubbles/droplets. The criteria and the surfactants that is more suitable for this process will be explained later in a subsequent paper. For the limited number of tests using this specific surfactant spontaneous nucleation was observed only when CO₂ was in liquid form.

CONCLUSIONS

1. “Spontaneous generation of droplets of CO₂-emulsion” was identified and introduced in this paper as an effective mechanism of bubble/droplet generation which can significantly improve strength (resistance to flow) of CO₂-emulsion in porous media.
2. This mechanism is not adversely affected by presence of oil. On the contrary, the rate of formation of CO₂ droplets increases when oil is present in the porous media.
3. This mechanism is not dependent on the fluid velocity or pressure gradient in the system. This makes this mechanism effective deep in the reservoir where all other bubble/droplet generation mechanisms are inadequate due to low fluid velocity and high oil saturation.
4. The core flood tests show significantly higher apparent viscosity in porous media for CO₂-emulsion systems in which spontaneous generation of CO₂ bubbles/droplets take place.
5. The coreflood tests show significant additional oil recovery and effective mobility control at high oil saturation in the system where spontaneous formation of CO₂ bubbles/droplets is active.

ACKNOWLEDGMENT

This work was carried out as part of the ongoing Enhanced Heavy Oil Recovery joint industry project (JIP) in the Centre of Enhanced Oil Recovery and CO₂ Solutions of Heriot-Watt University and was equally supported by: Total, ConocoPhillips, Pemex and Wintershall, which are gratefully acknowledged.

REFERENCES

1. Chambers, K.T. and Radke, C.J., 1990. “Capillary Phenomena in Foam Flow Through Porous Media”. In: Morrow, N.R.S (Ed.): “Interfacial Phenomena in Oil Recovery”, Surfactant Science Series, 191-256.
2. Chen, M., Yortsos, Y.C. And Rossen, W.R., 2006. “Pore-Network Study of the Mechanisms of Foam Generation in Porous Media”, Physical Review E, vol. 73, 181-189.
3. Emadi, A., Sohrabi, M., Farzaneh, S., Ireland, S., 2013. “Experimental Investigation of Liquid-CO₂ and CO₂-Emulsion Application for Enhanced Heavy Oil Recovery”, SPE/EAGE Europec, London, United Kingdom, 10–13 June 2013 (SPE-164798).
4. Klins, M. A. And Bardon, C. P., 1991. “Carbon Dioxide Flooding”. In: M. Baviere (Ed.): “Basic Concepts in Enhanced Oil Recovery Process”, Elsevier Applied Science.
5. Rossen, W.R., 1995. “Foams in Enhanced Oil Recovery”. In: Prud'homme, R.K. and Khan, S.A. (Eds.): “Foams: theory, measurements, and applications”, Marcel Dekker Inc.
6. Rossen W. R. and Gauglitz P. A., 1990 - "Percolation Theory of Creation and Mobilization of Foams in Porous Media," AIChE J.36, 1176.
7. Schramm, L.L. and Novosad, J.J., 1990. “Micro-Visualization of Foam Interactions with a Crude Oil. Colloids and Surfaces”, vol. 46, 21-43.
8. Sohrabi, M., Henderson, G.D., Tehrani, D.H. and Danesh, A., 2000. “Visualisation of Oil Recovery by Water Alternating Gas (WAG) Injection Using High Pressure Micromodels - Water-Wet System”, SPE Annual Technical Conference and Exhibition. Dallas, Texas, USA (SPE 63000).

9. Svorstol, I., Vassenden, F., and Mannhardt, K., 1996. "Laboratory studies for design of a foam pilot in the Snorre field", SPE/DOE Improved Oil Recovery Symposium, Tulsa, Oklahoma, 21-24 April 1996 (SPE 35400).

Table 1: Dimensions of the micromodel and its pores.

Height cm	Width cm	Pv cm3	Ave. depth μm	Pore Dia. Range μm
4	0.7	0.01	50	30-500

Table 2: Basic properties of the core sample used in this study.

Parameter	Size	Unit
Weight	1299.9	g
Diameter	5.12	c
Length	32	c
Core Pore Volume (PV)	163.02	c ³
Porosity (ϕ)	24.74	%
Permeability to Brine (K)	2.5	Darcy

Table 3: Basic properties of the heavy crude oil used for the micromodel and coreflood experiments.

API (°)	Asphaltene Content (%)	Acid Number (mgKOH/g)	Density @ 28 °C (g/ c3)	Dead Oil Viscosity @ 28 °C (cp)
16	2.60	0.94	0.93	617

Table 4: List of Coreflood tests.

Test No	Description	Press & Temp	Phases
1	CO2 Foam Flow	600 psig & 28 C	Vapour CO2, Surfactant
2	CO2 Foam Flow	1500 psig & 50 C	SC CO2, Surfactant
3	CO2 Emulsion Flow	1500 psig & 28 C	Liquid CO2, Surfactant
4	Oil Recovery by CO2 emulsion	1500 psig & 28 C	Liquid CO2, Surfactant, oil
5	Oil Recovery by liquid CO2	1500 psig & 28 C	Liquid CO2, brine, oil

Table 5: List of Micromodel tests.

Test No	Description	Press & Temp	Phases
1	CO2 Foam Flow	600 psig & 28 C	Vapour CO2, Surfactant
2	CO2 Foam Flow	1500 psig & 50 C	SC CO2, Surfactant
3	CO2 Emulsion Flow	1500 psig & 28 C	Liquid CO2, Surfactant
4	Oil Recovery by CO2 emulsion	1500 psig & 28 C	Liquid CO2, Surfactant, oil

Table 6: Basic properties of CO2 at different pressures and temperatures.

	Temp. (°C)	Press. (psig)	State	Density (g/ml)	Viscosity (cp)
CO2	28	600	Vapour	0.1	0.016
CO2	50	1500	Super-Critical	0.44	0.032
CO2	28	1500	Liquid	0.82	0.075
Water	28	1500	Liquid	1.00	0.888

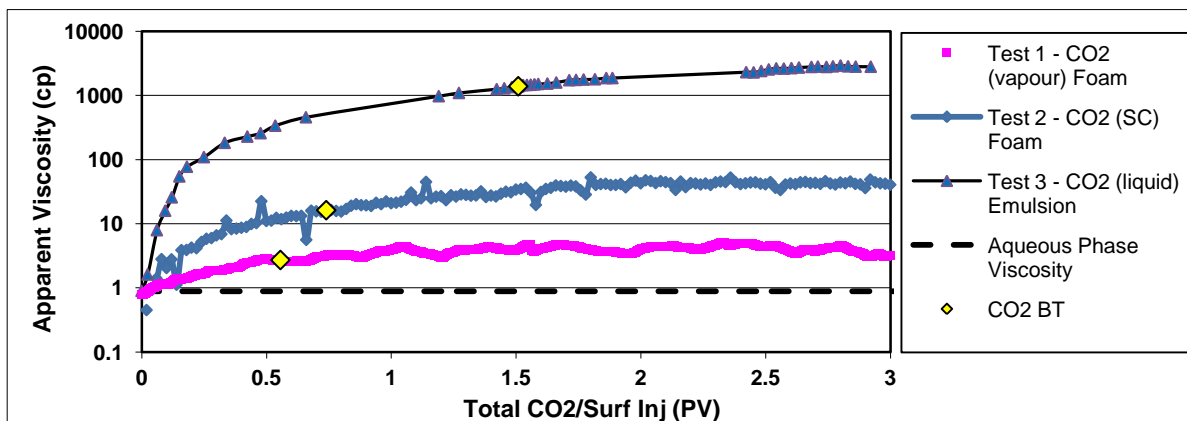


Figure 1: Apparent viscosity of CO2 foam/emulsion as a result of simultaneous injection of CO2 in vapour, SC and liquid forms and surfactant solution in absence of oil.

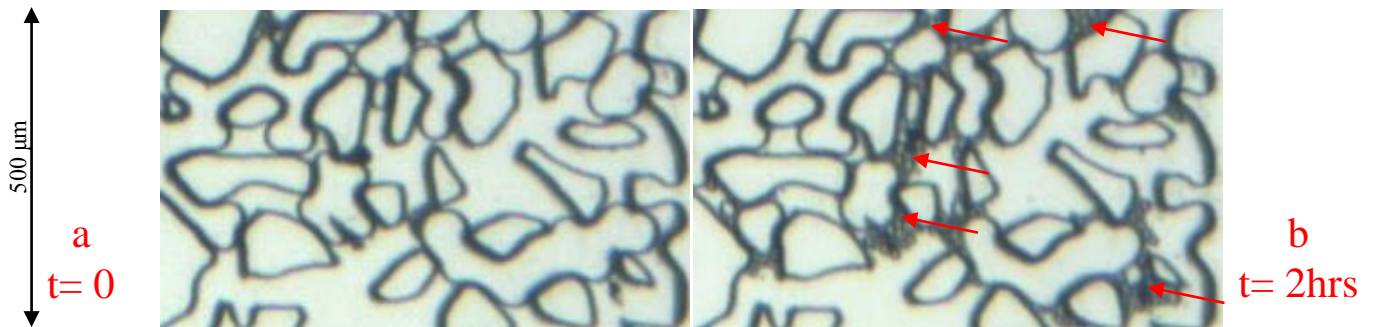


Figure 2: Spontaneous generation of CO2 emulsions (red arrows) in HW-A surfactant after 2 hours in no flow conditions (micromodel test 3).

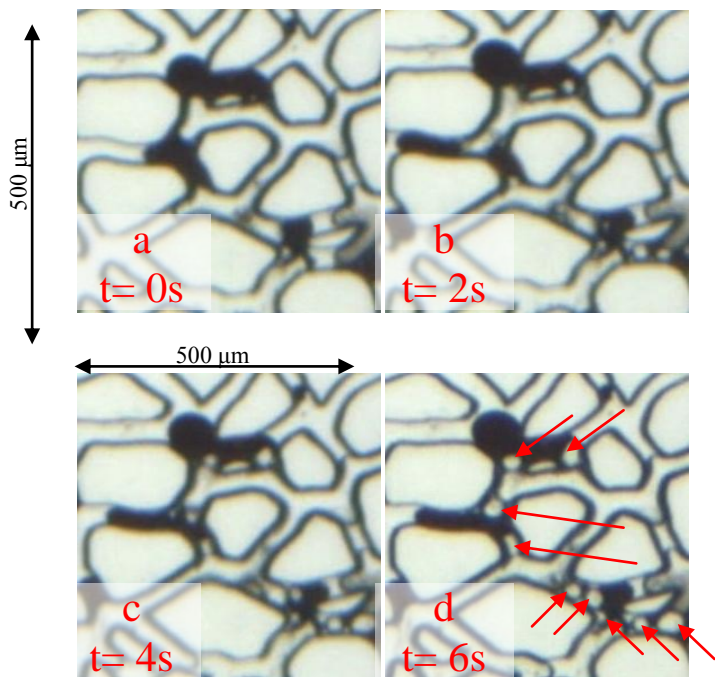


Figure 3: A sequence of images from a highly magnified section of the micromodel which show spontaneous formation of nine bubbles of CO2 emulsions at the oil/surfactant solution interfaces in only six seconds (micromodel test4).

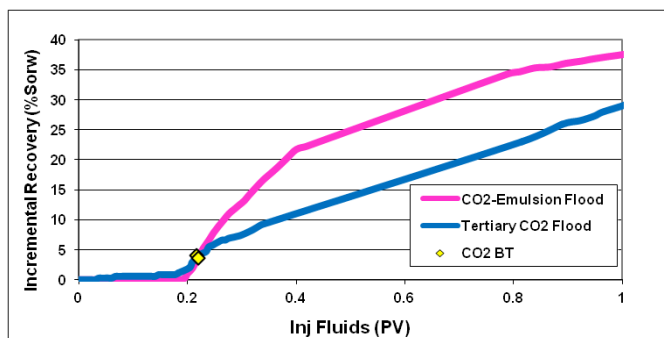


Figure 6: Comparison of the incremental oil recovery (based on waterflood remaining oil saturation) during CO2/surfactant co-injection in test 4 and tertiary CO2 injection in test 5.

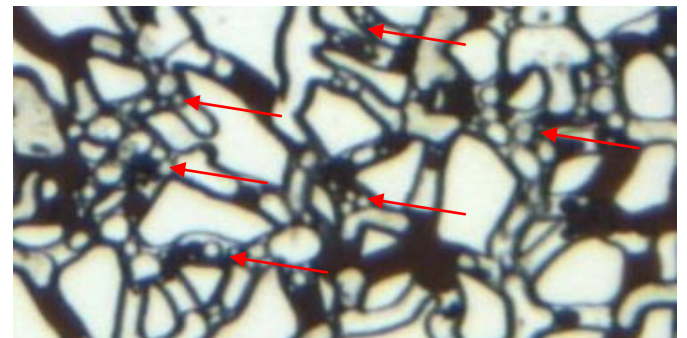


Figure 4: Spontaneous generation of a large number of CO2 droplets at CO2-emulsion front in presence of residual oil (micromodel test 4).

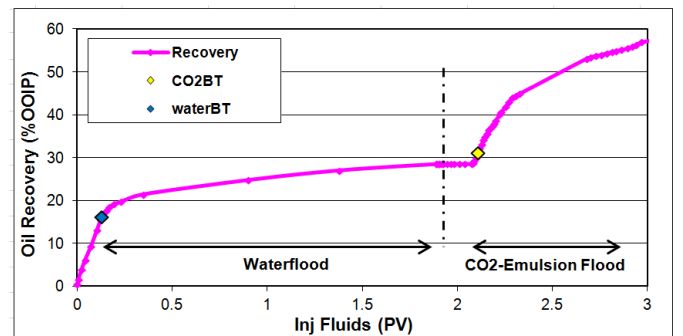


Figure 5: Cumulative oil recovery curve at different stages of coreflood test 4 including initial waterflood and subsequent CO2-emulsion injection.

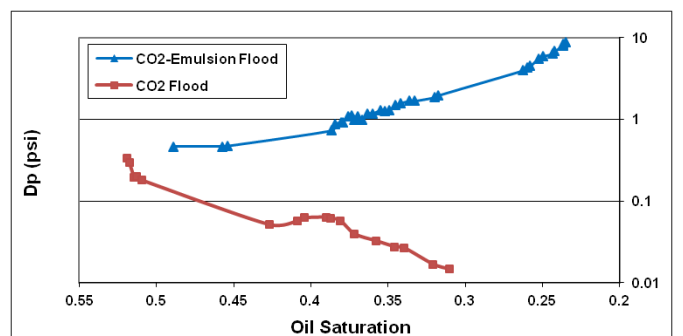


Figure 7: Comparison of the differential pressure in the core during CO2/surfactant co-injection in test 4 and tertiary CO2 injection in test 5 as function of residual oil saturation.